

ACCRETION DISKS IN INTERACTING BINARIES: SIMULATIONS OF THE STREAM-DISK IMPACT

P.J. Armitage¹

M. Livio²

ABSTRACT

We investigate the impact between the gas stream from the inner Lagrangian point and the accretion disk in interacting binaries, using three dimensional Smooth Particle Hydrodynamics simulations. We find that a significant fraction of the stream material can ricochet off the disk edge and overflow towards smaller radii, and that this generates pronounced non-axisymmetric structure in the absorption column towards the central object. We discuss the implications of our results for observations and time-dependent models of low-mass X-ray binaries, cataclysmic variables and supersoft X-ray sources.

ApJ accepted

¹Institute of Astronomy, Madingley Road, Cambridge, CB3 0HA, UK

²Space Telescope Science Institute, 3700 San Martin Drive, Baltimore, MD 21218, USA.

1. INTRODUCTION

Accretion disks in interacting binaries are unlikely to have simple axisymmetric structures. In these systems, the accretion disk is fed with material from a companion star via an accretion stream that originates at the inner Lagrange point. In this picture, both the gravitational influence of the companion and the impact of the stream with the disk provide mechanisms that may distort the shape and vertical structure of the accretion disk. Modeling of these deviations from axial symmetry requires the use of two and three dimensional hydrodynamic models, and is necessary in order to interpret a variety of observations of cataclysmic variables (CVs), low-mass X-ray binaries (LMXBs) and supersoft x-ray sources (SSS).

The X-ray light curves of nearly edge-on LMXBs provide one observational clue to the existence of non-axisymmetric disk structures. The eclipses are typically broad, with a gradual ingress that commences well before the phase of first contact (*e.g.* White *et al.* 1994). In some sources (“dipping” sources), most notably X1822-371, there is an actual dip in the flux at an orbital phase near 0.8. This absorption has been interpreted as arising from a bulge in the height of the disk rim at that phase (White & Holt 1982; Mason 1989 and references therein), which is suggestively similar to the location at which the accretion stream would impact the disk edge. X-ray observations of GK Persei (Hellier & Livio 1994) and EUVE observations of CVs (Warren, Sirk & Vallergera 1995; Long *et al.* 1996) provide further evidence for observational signatures of the accretion stream and its interaction with the disk.

Two dimensional calculations of accretion disk structure have primarily been used to investigate the formation of the disk and its response to the tidal field of the companion (Lin & Pringle 1976; Whitehurst 1988a,b; Lubow 1991; Murray 1996). Using a variety of particle-based numerical schemes, these studies show that for systems with a low mass ratio of secondary to primary ($q \lesssim 0.25$), the accretion disk is tidally unstable, leading to the formation of an eccentric precessing disk. Proper consideration of the effect of the accretion stream on the disk (which acts to add low specific angular momentum material at the outer edge and so tends to reduce the disk radius) shows that this modifies the phenomenon but does not alter the general behaviour (Murray 1996).

Hirose, Osaki & Minishige (1991) carried out simplified three dimensional calculations in an attempt to examine whether variations in disk scale height caused by the stream impact could explain the dipping X-ray sources. They found thickenings of the disk at around the phases expected, if these were the causes of modulation in the X-ray light curves. However, the difficulties of modeling the entire disk for many dynamical times meant that the resolution of the stream-disk impact region in this calculation was poor, and the authors commented that an improved treatment of the hydrodynamics beyond their “sticky particle” scheme was desirable. Much better resolution of the impact region was achieved in calculations by Livio, Soker & Dgani (1986) and Dgani, Livio & Soker (1989), but this was achieved at the expense of considering only a small region surrounding the point where the stream met the disk. Thus, while these calculations

demonstrated clearly the flow pattern in the collision region, there remained the possibility that the hydrostatic vertical structure assumed for the disk gas might not be realistic, if the response of the entire disk to the stream was included. With this caveat, however, the calculations did demonstrate that stream material could overflow the disk rim, as suggested by the work of Lubow & Shu (1975, 1976), Lubow (1989) and Frank, King & Lasota (1987).

In the current investigation, we extend these studies by performing three dimensional Smooth Particle Hydrodynamics (SPH) simulations of the response of the disk to the accretion stream. We focus on the dynamical effects of the stream-disk collision – for which the SPH method is well-suited – and aim for the highest practicable resolution of the interaction region. We do not attempt to model the thermal or long-term viscous evolution of the disk, for which purpose other numerical techniques would be preferable. By ignoring these aspects we are able to improve the resolution of the stream-disk impact region when compared, for example, to prior 3D simulations by Lanzafame, Belvedere & Molteni (1994a, 1994b), who were interested primarily in modeling outburst behaviour over longer timescales than those considered here.

The layout of this paper is as follows. In Section 2 we describe the computational methods and binary system parameters that we adopt for the simulations. Section 3 presents and interprets the results of the calculations, while Section 4 summarizes our conclusions and suggests further observational tests of the models.

2. COMPUTATIONAL APPROACH

2.1. Smooth Particle Hydrodynamics

The simulations described in this paper were performed using a three dimensional SPH code minimally modified from that described by Benz (1990). SPH is a fully lagrangian, particle-based hydrodynamics method, that has been applied to a wide variety of problems in astrophysics (see, *e.g.* Monaghan 1992), and has been shown to give closely comparable results to hydrodynamics codes based on alternative numerical techniques (*e.g.* PPM—Davies *et al.* 1993).

For the simulation of accretion disks, SPH has a number of advantages. A Keplerian disk exhibits a rapid variation of dynamical timescale with radius, which is computationally expensive if the problem demands that a significant range of radii be modeled. This difficulty can be partially alleviated in an SPH calculation by assigning each particle its own timestep satisfying the Courant stability criterion, so that the bulk of the disk material at relatively large radii can be integrated on a longer timestep. SPH has further merits in facilitating easy tracing of the flow, and in not wasting resources following the void regions outside and above the accretion disk.

Disadvantages of this method include the variable resolution of an SPH calculation, which is worst in the low density parts of the flow where the particle density is small. As these regions—well

above the mid-plane of the disk—are precisely those that are most important for determining the X-ray and EUV absorption, this is a potentially serious problem. We mitigate its effect by exploiting the freedom that SPH allows in setting particle masses, so that the stream particles (which on collision with the disk will form the majority of the material high above the disk plane) have lower masses than those in the disk. More problematic is the fact that our code neglects the effects of radiation transport and cooling of the gas, so that the only control over the thermal properties arises via the choice of the equation of state. We adopt an isothermal equation of state, which corresponds to assuming that the energy generated from viscous and shock heating is radiated away instantaneously. For a standard α accretion disk (Shakura & Sunyaev 1973), the thermal timescale, $t_{\text{th}} \sim \alpha^{-1}\Omega^{-1}$, is comparable to the dynamical timescale, $t_{\text{dyn}} \sim \Omega^{-1}$, if the Shakura-Sunyaev viscosity parameter α is of order unity (Pringle 1981). Arguments based on the timescales involved in the outbursts in these systems suggest that for CVs and LMXBs α is typically in the range 0.1–1, so that the isothermal equation of state provides a reasonable approximation to the much more complicated physics that is actually involved. Caution is nevertheless required in interpreting our results close to where shocks—and hence strong and rapid heating of the gas—occur in the simulations.

2.2. System Parameters

Having ignored both thermal and viscous effects, the important system parameters that remain are the mass ratio $q = M_2/M_1$, the disk mass M_{disk} , and the accretion rate \dot{M} . For low mass ratios $q \lesssim 0.25$, prior calculations show the formation of an eccentric, tidally unstable disk, which precesses in the rotating frame of the binary (Whitehurst 1988a,b; Lubow 1991). Such mass ratios are likely to be relevant both to subclasses of dwarf novae (the SU UMa systems), and to many LMXBs with low-mass (a few tenths M_{\odot}) companions. Conversely, higher mass ratios lead only to a modestly distorted disk which remains fixed in the Roche frame of the binary.

The disk mass and accretion rate are expected to be significant mainly via the combination $f = \dot{M}P/M_{\text{disk}}$, where P is the period of the binary. f is then the fraction of the disk mass that is replenished per orbit, and it measures how strong a perturbation the stream can exert on the disk. To estimate sensible values for f , we assume a Shakura-Sunyaev disk in which the viscosity is given by $\nu = \alpha c_s H$, where c_s is the sound speed and $H \approx c_s/\Omega$ is the disk scale height. For such a disk, the surface density Σ in the steady state is given by,

$$\nu\Sigma = \frac{\dot{M}}{3\pi}, \quad (1)$$

for radii much larger than the inner disk radius. Taking $M_{\text{disk}} \sim \pi R^2 \Sigma$, we then obtain an estimate for f ,

$$f = \frac{\dot{M}P}{M_{\text{disk}}} \sim 6\pi\alpha \left(\frac{c_s}{v_K} \right)^2, \quad (2)$$

where v_K is the Keplerian velocity in the disk and all quantities are evaluated at the disk edge. For a thin disk $c_s/v_K \ll 1$ (≈ 0.03 for our simulations), so that f is small, typically of order 10^{-2} , even for α of order unity. This is also consistent with the timescales of outbursts (in which mass accumulated in the disk over an extended time rapidly drains onto the central star), which generally last $\sim 10^2 P$.

In previous calculations the most dramatic effects of the companion on the accretion disk were found to occur for low mass ratios. We therefore adopt $q = 0.2$, as appropriate for a $0.3 M_\odot$ companion to a $1.4 M_\odot$ primary, and $f = 0.025$. For the particular value of M_{disk} in the calculations, this corresponds to a mass transfer rate of $\dot{M} = 2 \times 10^{17} \text{ gs}^{-1}$, or $3 \times 10^{-9} M_\odot \text{ yr}^{-1}$ (run LMXB2). To assist in disentangling the effects of the Roche potential from those caused solely by the impact of the stream, a second simulation was run with a very low mass secondary (q effectively zero), and otherwise similar values of disk mass and accretion rate (run LMXB1).

2.3. Disk and Stream Set Up

As we have already remarked, simulating the innermost regions of the disk is computationally prohibitive. Fortunately it is also unnecessary, since on a dynamical timescale the stream is unable to influence the disk interior to the stream circularization radius. We therefore set up the disk as an annulus with an inner edge at approximately the circularization radius and an outer edge at the tidal truncation radius as given by Papaloizou & Pringle (1977) and Paczyński (1977). To prevent a small fraction of particles from bringing the simulation to a halt by moving too far inward under the action of viscosity, we add angular momentum to any disk particle straying inside a radius R_{bound} from the primary. For the runs described here, R_{bound} is set at half the inner radius of the annulus. Over the relatively short timescale of our runs, we observe no effect of this inner boundary condition on the disk annulus farther out.

Although the effects of *physical* viscosity are unimportant for these calculations, it is important that the artificial viscosity in the code, parameterized by α_{SPH} and β_{SPH} (Benz 1990), is sufficient to prevent particle interpenetration in the shocks that occur when the stream strikes the disk edge. An isothermal equation of state provides the least resistance to particle interpenetration (as there is no shock heating to generate additional pressure gradients), and so we adopt the rather high values $\alpha_{\text{SPH}} = 2$, $\beta_{\text{SPH}} = 4$. Previous work (Bate 1995) has shown that this should be adequate to stop particles streaming past each other, and we do not see any such behaviour in our runs. The internal SPH viscosities can be converted into a physical Shakura-Sunyaev α parameter via the formula (*e.g.* Bate 1996),

$$\alpha \approx \left(\frac{\alpha_{\text{SPH}}}{20} \right) \left(\frac{h}{H} \right), \quad (3)$$

where h is the particle smoothing length in the simulation (3D). The β -viscosity will also have some effect, but for a disk that is resolved in the vertical direction, the contribution to the

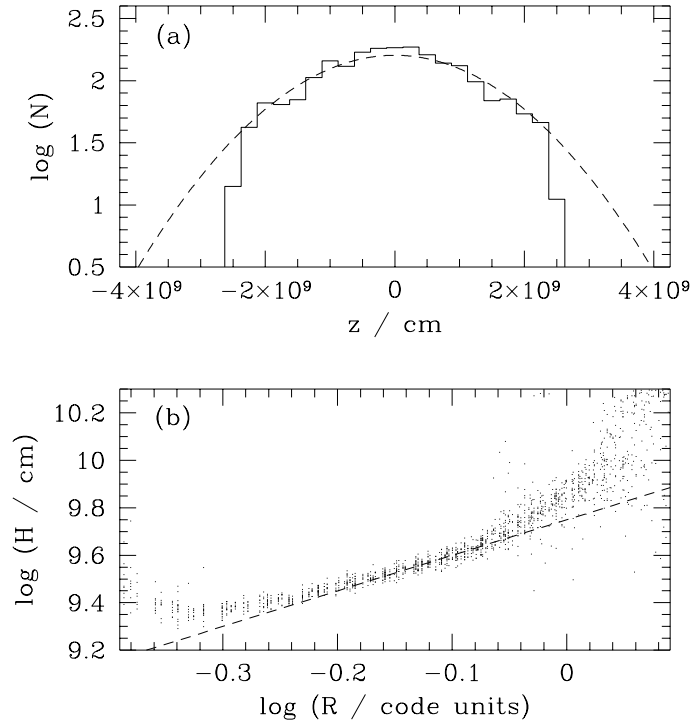


Fig. 1.— (a) Distribution of particles in z for a thin annulus in a quiescent (no stream) disk. The dashed line shows a gaussian distribution with width $\Delta z = 2 \times 10^9$ cm. (b) The disk scale height evaluated in cells for the same quiescent disk, plotted as a function of radius. The dashed line represents $H \propto R^{3/2}$.

kinematic viscosity from the second-order β_{SPH} term will be smaller than that from α_{SPH} (Bate 1996). Using this expression it can be seen that for simulations that are resolved vertically ($h < H$, as in our calculations), typical SPH viscosity parameters lead to values of α that are smaller than those believed to pertain to CV and LMXB accretion disks, and there should be no problems arising from unreasonably large artificial viscosity in the simulations.

The disk gas is modeled using 30000 equal mass particles that are initially distributed on a close-packed lattice within 2.5° of the disk plane, and which have Keplerian velocities about the primary. The sound speed is set such that $c_s/v_K = 0.03$ at the outer edge of the disk—this gives a somewhat thicker disk than is usually assumed, but has the advantage that better resolution is attained in the vertical direction. The disk reaches a stable hydrostatic equilibrium structure quickly (in less than one orbit), after which the distribution of particles with z (perpendicular to the disk) for a narrow annulus of disk is as shown in Fig. 1(a). The particles follow a gaussian distribution, as expected for an isothermal accretion disk, and track the density profile well, up to the height where the particle number density becomes very low. Calculating the disk scale height

(defined as $H = \Sigma/\rho_{z=0}$, where Σ and $\rho_{z=0}$ are evaluated from the SPH calculation) as a function of radius yields the results shown in Fig. 1(b). For an isothermal disk, $H \propto c_s/\Omega \propto R^{3/2}$, and this scaling is shown in the Figure as the dashed line. Over the range ($-0.3 < \log(R) < 0$) where the disk is resolved vertically this relation is found to be obeyed, with discrepancies at the inner and outer edges where the particle density is dropping off rapidly.

For run LMXB2 the presence of the companion means that the disk is not being set up with velocities that are consistent with disk orbits in the binary potential. To allow time for these initial conditions to be smoothed out, the disk is first evolved for ~ 10 orbits of the binary before the stream flow is switched on. During this relaxation period the disk develops a stable but distorted shape, with a smooth variation of surface density. For the purposes of the present work this represents well enough the ‘background’ disk structure onto which the stream flows, though if, for example, one wished to follow the disk precession in a 3D calculation, a more elaborate disk set up would certainly be desirable.

For the initial conditions of the stream, we utilise the results of Lubow & Shu (1975, 1976), see also review by Livio (1994). These show that the width of the stream, W , in both the azimuthal and vertical directions, is given approximately by,

$$W \sim \frac{c_s}{\Omega_{\text{binary}}}, \quad (4)$$

where c_s is here the sound speed at the surface of the mass-losing star and Ω_{binary} is the binary angular velocity. This is essentially the same relation as for the disk scale height, and implies that the stream is much thicker than the pressure scale height of the mass-donating star H_* (indeed, $W \sim \sqrt{H_* R_*}$).

Numerically, the stream is modeled as a tube of particles stretching outward from the inner Lagrange point, L_1 , with radial velocities set to be c_s towards the primary. When a particle passes inward of L_1 (towards the primary) it is added to the simulation and evolved under the influence of gravity and all hydrodynamic forces, while particles outside L_1 are simply rotated to follow the binary orbit. Initially the stream particles are strongly compressed in the radial direction (by a factor ~ 10). This ensures that when the stream reaches the disk edge the separations are comparable in R and in z , as required to model the impact hydrodynamics. We assume that the stream leaves L_1 in hydrostatic equilibrium, and set the vertical density profile to be a gaussian with width W . This is truncated at 1 scale height, where the scale height is estimated by extrapolating the numerical results obtained from the disk (Fig. 1), and allowing, where necessary, for the gravity of the secondary. The compression required in R near L_1 means that the stream there is not in numerical hydrostatic equilibrium, but this is of no consequence, since the stream flow toward the disk is ballistic. The simulations follow the stream-disk interaction for around 2-3 orbits of the outer disk, requiring 20000–30000 particles to achieve adequate resolution of the accretion stream.

Fig. 2.— Particle distribution in the $x - y$ and $x - z$ planes for simulation LMXB2 (mass ratio of secondary to primary $q = 0.2$). This figure is omitted due to size, and is available from <http://www.ast.cam.ac.uk/~parm/lmxb.html>

3. RESULTS

3.1. Stream Overflow

Fig. 2 shows a snapshot of particle positions during the latter stages of run LMXB2. For both simulations, a quasi-steady state appearance in the Roche frame is rapidly attained, so that although the disk mass is slowly increasing throughout, successive snapshots look very similar. Where the stream reaches the disk, the Figure shows that the oblique collision both shears the stream and compresses the disk edge. Some stream material is transferring its momentum to the disk gas and becoming buried in the disk rim. This is similar to the behaviour seen in previous calculations (*e.g.* Livio *et al.* 1986; Rozyczka & Schwarzberg-Czerny 1987). However, from the $x - z$ projection it is also clear that some stream gas is overflowing the disk rim as a result of the collision. This material is being thrown to larger distances above the midplane than the original stream, and is many scale heights above the disk itself.

To clarify the origin of this overflowing gas, we plot in Fig. 3 density contours in a vertical plane, aligned along the direction of the accretion stream flow where it reaches the disk edge. We also show velocity vectors in this plane for the stream gas, calculated by simple averaging of particle velocities in spheres of radius $2h$. Although the disk in general flares towards large radius ($H \propto R^{3/2}$), it can be seen that in the outermost regions of the disk where the surface density is dropping, the density contours form a wedge-like structure. The stream strikes this supersonically, and the outer parts ricochet off to greater distances from the disk midplane. This behavior has been predicted by the analytic Sedov Solution obtained by Livio *et al.* (1986). The vertical velocities away from the $z = 0$ plane that are achieved in this manner, are typically several times c_s , so this gas reaches a maximum $|z|$ that is many times the disk scale height. Further downstream the overflowing gas falls back to the disk, achieving higher velocities than on impact, because now it is closer to the primary where the vertical component of gravity is greater. While the central core of the stream tends to blunt the wedge, it is continually restored by fresh disk material that possesses a higher angular velocity than the orbital one.

3.2. Density Slices from the Simulations

Figs. 4 and 5 show the density calculated using the SPH smoothing algorithm for both simulations. We plot the midplane density, panel (a), and the density at a few scale heights above

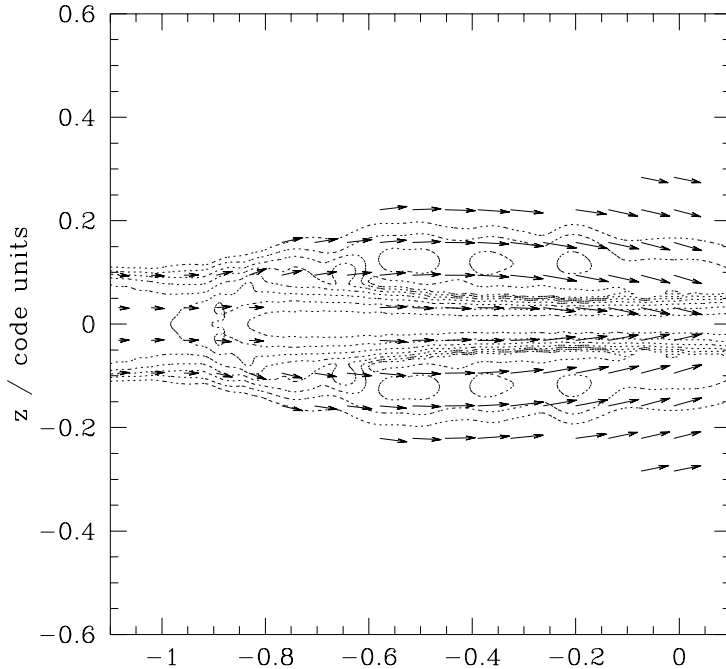


Fig. 3.— Logarithmic density contours (dashed lines) in a vertical plane aligned with the direction of stream flow at the location where the stream strikes the disk. Vectors represent the velocity in this plane of stream material. The z -component of the velocity vectors has been enhanced by a factor of two for clarity.

the midplane, panel (b). In the latter plot, we have co-added 4 independent time-slices in order to reduce the Poisson noise due to limited particle number, though the behavior we describe is clearly seen also in individual snapshots. For both simulations the compression of the disk rim due to the momentum of the stream impact is evident (the oscillations in radius of the disk, downstream of the impact, are probably due to remaining anisotropies in particle distribution on impact, and are not physical). However, except for this, the midplane density plots show little structure beyond what would be expected given the initial set up of these disks.

At high $|z|$, conversely, strong signatures of the stream impact are visible. For LMXB1 a single region of relatively high density is obtained, beginning at the point where the stream reaches the disk and persisting until around phase 0.75 (here phases are measured with respect to the phase at which an eclipse would occur, and increase clockwise in the plots). This peak lies well inside the outer edge of the disk, and arises from the overflowing stream material discussed earlier. Although the resolution at this z is limited by relatively small particle numbers, it appears that the overflowing gas does *not* form a well-collimated continuation of the accretion stream. Rather

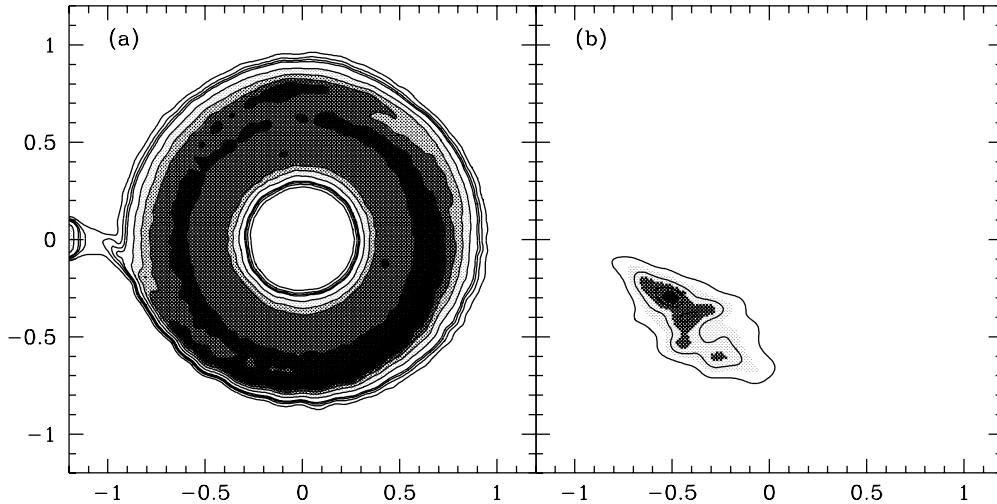


Fig. 4.— Density from simulation LMXB1 (secondary of zero mass) in the $x-y$ plane at (a) $z = 0$, and (b) $z = 0.15$.

the impact leads to a broad fan of material ejected to high $|z|$ as a consequence of the collision.

For the simulation with the full Roche potential, a similar structure generated by the stream-disk interaction is seen in the density plots. In this instance however, a second broad and comparatively high density region is seen at phase 0.2, which originates from the eccentricity of the accretion disk in this simulation. The disk is flared, and so for a given high z slice, the greatest density contribution is expected to come from material at the largest radius. This leads to a peak roughly in the direction along which the disk is most extended, though from the simulation the peak is seen at a somewhat earlier phase, probably as a consequence of the disk gas not reaching hydrostatic equilibrium and hence lagging in adjusting to the changing vertical gravity. We note that the magnitude of the second peak is probably overestimated by the simulation, as the SPH particles at the outer edge of the disk have no neighbours at greater radii and so adopt larger smoothing lengths to maintain a roughly constant number of neighbours. These larger smoothing lengths will enhance the density contribution at high $|z|$. When this numerical effect is borne in mind, both simulations demonstrate that material directly thrown above the midplane by the stream-disk impact is likely to dominate the absorption column at high $|z|$.

3.3. Column Densities Towards the Primary

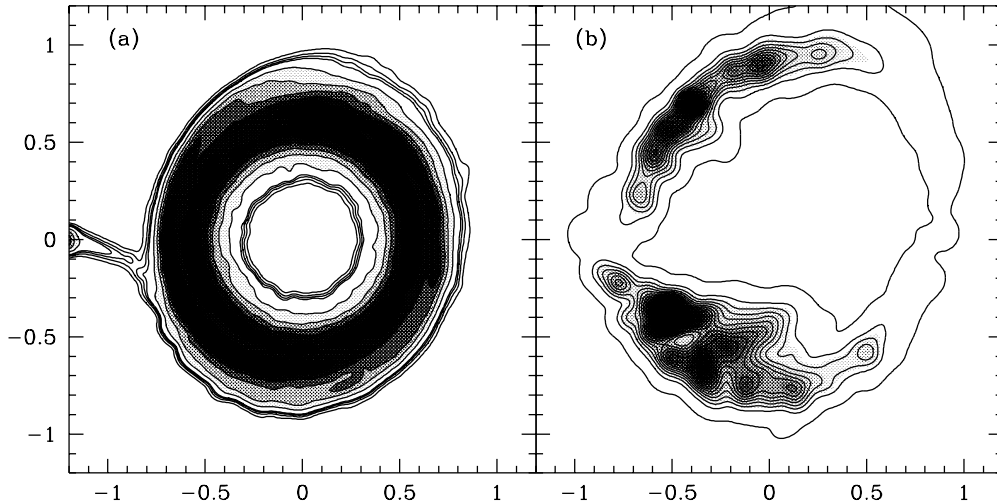


Fig. 5.— Density from simulation LMXB2 (full Roche potential, $q = 0.2$) in the $x - y$ plane at (a) $z = 0$, and (b) $z = 0.12$.

In order to quantify the observable effects of the material thrown out of the plane we have calculated the column density σ along various lines of sight toward the primary from our simulations. We calculate,

$$\sigma(\phi, \theta) = \int \rho dl \quad (5)$$

from integration of the SPH density estimator along lines of sight toward the primary at phase ϕ and at angle θ above the disk midplane. ϕ values are chosen so that neighbouring lines of sight are calculated from different sets of particles and hence independent. As the innermost particles have overly large smoothing lengths for the reasons already discussed, these are removed before column densities are calculated. This cut affects only $\sim 1\%$ of the particles.

Fig. 6 shows the results for both simulations, for angles of elevation $\theta = 0, 6, 12^\circ$. For comparison, the dipping source X1822-371 is believed to be viewed at an inclination angle of $82^\circ - 87^\circ$ (Mason 1989). For LMXB1 there is no variation evident above the noise at $\theta = 0^\circ$. By $\theta = 6^\circ$ the overflowing stream material, seen in Fig. 4 at high $|z|$, is producing a significant contribution to the column density, leading to a peak in σ at phase $\phi \sim 0.8$. There is marginal evidence for a broad feature also at $\phi \sim 0.2$, caused by the compressed disk rim expanding outwards downstream of the stream impact point. However, at the highest angle of elevation, $\theta = 12^\circ$, the overflowing stream gas provides the *only* source of absorbing column, and there is a single strong peak centred on $\phi = 0.85$ and extending from phase 0.7 through to eclipse. For an opacity generated solely by Thomson scattering a column density of order unity is required to produce an optical depth of 1, and hence for this accretion rate ($3 \times 10^{-9} M_\odot \text{ yr}^{-1}$) the overflowing

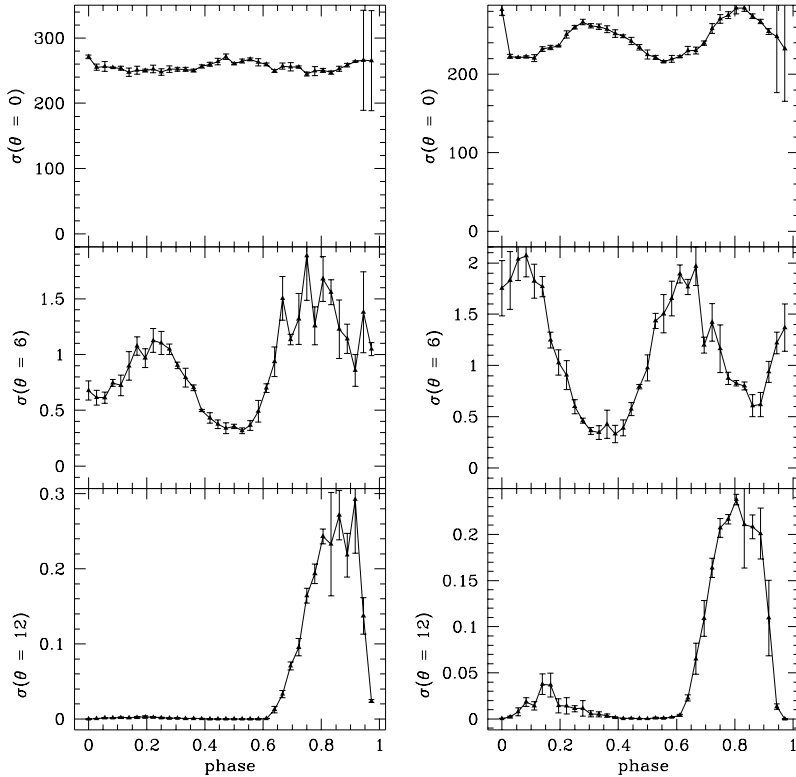


Fig. 6.— Column density σ towards the primary as a function of phase for varying angles of elevation above the disk plane $\theta = 0, 6, 12$ degrees. Left panels are for simulation LMXB1, right panels for LMXB2. Units are g cm^{-2} . Error bars are calculated from 4 independent time-slices of the simulations.

gas would be sufficient to create significant absorption even at angles to the midplane $\theta \gtrsim 10^\circ$.

For run LMXB2 the situation is more complicated. At $\theta = 12^\circ$ there is a single strong peak in column density at phase 0.8, which as before is associated with the stream-disk interaction. There may be a hint of a very small peak at $\phi \sim 0.1-0.2$. However in this simulation there is significant variation in σ with phase even at $\theta = 0^\circ$, as a result of the marked distortion of the disk shape under the gravitational influence of the companion. Of course viewed directly edge-on, the optical depth to the central object is enormous, and so the variation in this regime would not be observable. These variations suggest, however, that at intermediate viewing angles both effects should be important, and this is seen in the plot for $\theta = 6^\circ$, where two clear peaks are produced—one arising from the stream overflow and one from the disk structure. Since the disk precesses in the frame of the binary (for low q systems), the absorption feature arising solely from the eccentric disk structure should vary linearly in phase with time. Conversely, structures

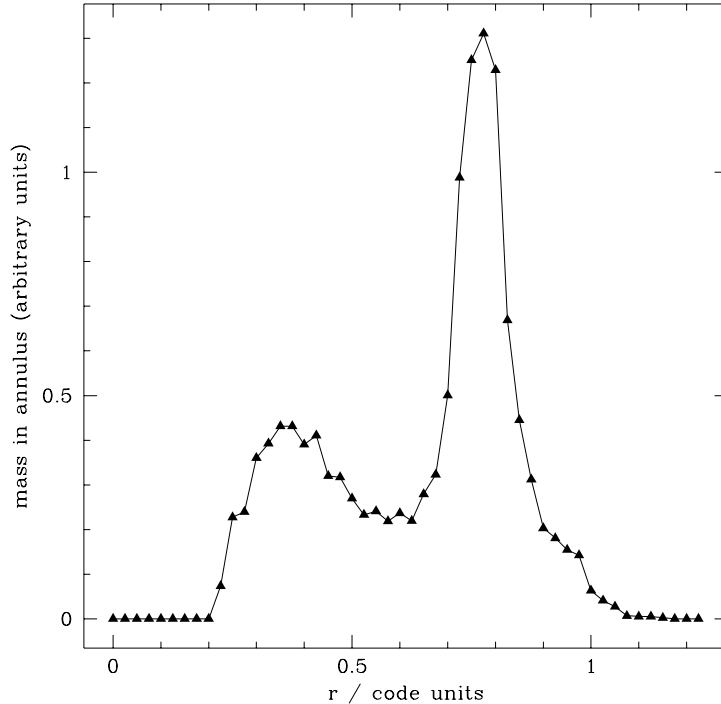


Fig. 7.— Destination of stream mass (in arbitrary units) as a function of radius.

generated directly by the stream-disk interaction should remain at fixed phases (regardless of the mass ratio of the binary).

3.4. Fate of Stream Material

Time-dependent models for accretion disks in (dwarf nova) systems vulnerable to thermal instability-driven outbursts generally add mass to the disk from the stream either in the outermost computational zone (*e.g.* Pringle, Verbunt & Wade 1986), or else with a narrow gaussian profile at the outer edge (*e.g.* Cannizzo 1993). Neither is likely to be a good representation of the physical situation if a significant fraction of the stream mass overflows the disk rim and circularises at smaller radii. To examine this possibility, Fig. 7 shows the destination of stream material as a function of radius in the disk, for simulation LMXB1, where the disk is circular and the complicating effects of an eccentric disk are not present. The distribution is bimodal, with most of the mass being deposited and circularising at the outer disk rim, but with a significant fraction ($\sim 1/3$) ending up at much smaller radii. The outer peak is caused by the dense inner core of the stream, which on impact with the disk becomes buried in the outer edge, while the inner peak

(near the stream circularisation radius) is formed from the stream gas that overflows the disk rim.

This result must be treated with some caution however, as the current simulations do not have sufficient resolution to resolve, for example, any surface instabilities that might entrain the overflowing stream gas more efficiently and thus keep it at larger radii. Calculations with a higher resolution and better treatment of the thermal properties of the gas will be required to investigate this possibility. The general picture from our simulations, however, is that neither mass addition exclusively at the outer edge nor mass addition primarily at the circularization radius is likely to prove a good approximation. Rather, the surface density increment is bimodal with roughly equal amplitudes at the two radii, and we anticipate that this is likely to alter the detailed behaviour seen in time-dependent disk instability models.

3.5. Location of energy dissipation

In our simulations artificial viscosity is used in the momentum equation to generate shocks and prevent particles streaming freely through each other. In the physical disk, these shocks would lead to strong heating of the gas, and create bright spots on the disk surface. The strength of this dissipation can be estimated by calculating the shock heating that would occur in the simulation if the gas had an adiabatic ($\gamma = 5/3$) equation of state, while the flow pattern remained as we have described.

Fig. 8 shows the energy dissipation estimated in this way as a function of phase, for annuli that cover the radial extent of the disk. For the annuli at smaller radii, the background level of dissipation is uniformly greater because of the increased viscous dissipation that is unconnected with shocks. Excesses over this level represent areas where bright spots might be expected to occur. As expected, the strongest dissipation is found in the outermost annulus, at the location where the stream strikes the disk. However there is also strong shock heating occurring in the innermost ring, at the location where the overflowing stream gas collides again with the disk (at phase $\phi \sim 0.6$). A smaller fraction of stream material reaches this radius, but being being deeper in the potential well the total shock heating is similar. No prominent features are seen in the two intermediate annuli.

The width of the features seen in Fig. 8 represents only the azimuthal extent of the regions where shock heating would occur, the actual size of the bright spots produced as the shocked gas cools will undoubtedly be much larger and may cover a sizeable fraction of the disk circumference (Rozyczka & Schwarzenberg-Czerny 1987). Our calculations suggest that a second bright spot should be formed at the roughly diametrically opposed phase where the overflowing gas returns to the disk plane. This inner bright spot is of comparable luminosity to that formed directly by the stream-disk impact, though relative to the background emission at the smaller radius it is, of course, much weaker. It would thus be most easily seen in systems with low viscosity (*e.g.*

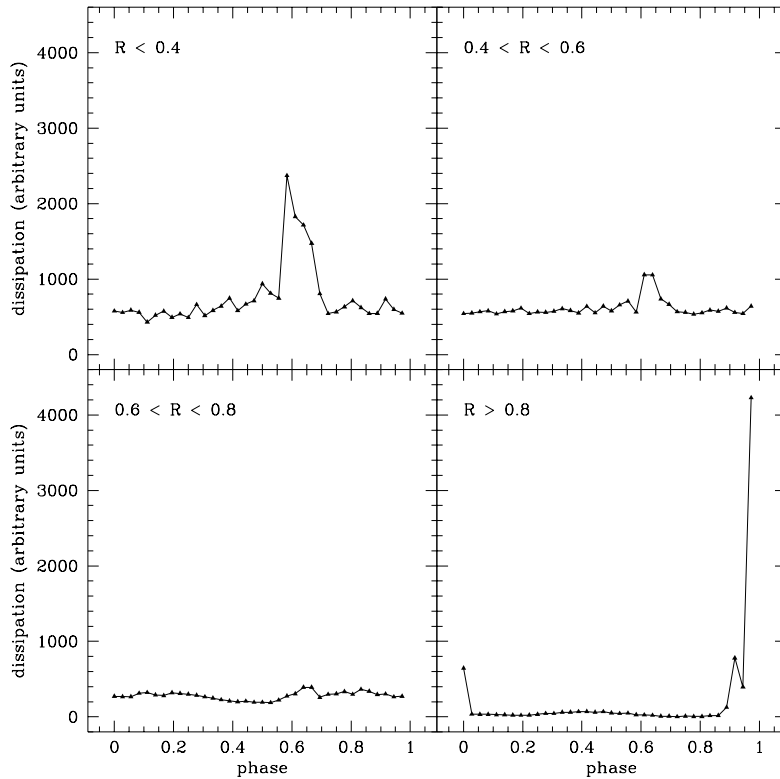


Fig. 8.— Rate of heating from shocks as a function of phase for annuli in the disk (simulation LMXB1). The panels run from the innermost annulus at upper left, to the outermost at bottom right. The disk edge is at $R \approx 0.9$ in these units.

dwarf novae with long recurrence times), and could provide valuable clues to the degree of stream overflow occurring in these systems.

4. SUMMARY AND DISCUSSION

We have presented three dimensional SPH calculations of the stream-disk interaction. The main conclusion to be drawn from these simulations is that significant amounts of stream material are able to overflow or bounce off the edge of the disk, and flow over the disk surface towards smaller radii. This creates a peak in the column density towards the primary at a phase of around 0.8, and is a likely cause of the absorption dips observed at around this phase in some nearly edge-on low-mass X-ray binaries (see *e.g.* review by White, Nagase, & Parmar 1995). If this is the case, the absorbing material is located (in radial distance) intermediate between the disk edge

and the stream circularization radius. At the highest angles of elevation above the disk surface ($\theta \gtrsim 10^\circ$), we see no significant absorbing column at any other phases. Recent EUVE observations of U Gem in outburst (Long *et al.* 1996) show an absorption dip (at phase ~ 0.75) caused by material a few scale heights above the disk surface, in complete agreement with the results of the present study. ASCA observations show that the dips persist in quiescence (Szkody *et al.* 1996).

This result differs from that of Hirose, Osaki & Minishige (1991), who in addition to predicting absorption at phase 0.8 also found absorption at phase 0.2 in their models (although as they did not compute column densities from their simplified calculation it is unclear whether both those features would be visible at large θ). We do find significant absorption at around phase 0.1–0.2 for lower angles of elevation above the disk plane, and this seems to be primarily due to the eccentricity induced in the disk by the gravity of the companion. We note that in low mass ratio systems absorption features generated by the eccentric disk structure should precess with the disk, and thus can be separated from those induced by the stream-disk interaction, which remain at a fixed phase (~ 0.8) regardless of the mass ratio. Therefore, in systems where two absorption features are seen, a straightforward observational test to determine their origin is possible, by monitoring for a prolonged period the phases of maximum absorption.

The presence of gas that is not in hydrostatic equilibrium flowing over the disk raises a number of intriguing possibilities. If exposed to an X-ray power-law spectrum from the central source, it may be prone to a two-phase instability and break up into dense clouds surrounded by a hot diffuse medium (Krolik, McKee & Tarter 1981; Frank, King & Lasota 1987). Such a picture might explain the very short-timescale variations seen in some dipping X-ray sources. Less speculatively, the wide range of radii over which mass from the stream circularises in our simulations, implies that significant changes might be expected in the behavior predicted from time-dependent thermal disk instability models. In particular, during quiescence, the quasi ballistic flow over the disk might dominate inflow caused by viscosity in the outer disk, and this would affect predictions for the behaviour of the disk radius. Significant stream overflow implies that less material with low specific angular momentum will be added at the outer edge of the disk, and hence less contraction of the disk radius during quiescence would be expected. If the degree of overflow were large (as might occur if the outer disk were cold relative to the mass-donating star), then substantive differences in the surface density profile during quiescence would also occur. This could lead, for example, to thermal instabilities triggered at intermediate disk radii, and other, detailed, differences to standard models.

For systems that undergo outbursts, the presence of overflowing stream gas provides a possible observational probe of the disk radius. As the disk expands, the phase of maximum absorption is expected to increase (closer to the phase of eclipse) as a consequence both of the position and angle at which the accretion stream reaches the disk. More subtle effects might also occur due to the varying temperature of the outer disk over the course of an outburst cycle. A hotter disk is thicker, and this should reduce the amount of stream material able to overflow the rim and thereby reduce the depth of the absorption. A thicker disk might of course absorb radiation from

the primary directly, but this effect would be axisymmetric and thus distinguishable from that caused by high $|z|$ stream gas. Simultaneously *more* energy would be dissipated in the bright spot at the disk rim, so that the bright spot luminosity would increase as the outburst commenced. There is some observational evidence that this brightening does occur (Livio 1994).

We should note that in their attempt to model the visual light curve of the eclipsing supersoft X-ray source CAL 87, Schandl, Meyer-Hofmeister, & Meyer (1996), found that they had to assume the presence of an optically thick “spray” of material around the disk. They conjectured that such a spray might form by the disk-stream interaction. An examination of Fig. 2 reveals that we indeed obtain a configuration similar to that assumed by Schandl *et al.* (1996).

Finally we remark that in this paper we have concentrated on explaining features seen in the X-ray and EUV wavebands. Important information is also available in the optical, especially from the analysis of time-resolved spectra using doppler tomography (Marsh & Horne 1988). Many systems have now been mapped using this technique (*e.g.* Kaitchuck *et al.* 1994), and in some cases the path of the accretion stream can be clearly traced. A future comparison of synthetic doppler maps generated from simulations of the type presented here with these data appear to provide a fruitful direction in which the research into stream-disk interactions can continue.

ACKNOWLEDGEMENTS

We thank Ian Bonnell, Cathie Clarke, Melvyn Davies, Andy Fabian, Steve Lubow and Donald Lynden-Bell for useful discussions and suggestions. PJA thanks Space Telescope Science Institute for hospitality. ML acknowledges support from NASA Grant NAGW-2678 at ST ScI, and thanks the Institute of Astronomy, Cambridge, for its hospitality.

REFERENCES

- Bate, M. 1995, Ph.D. Thesis, University of Cambridge, p. 43
- Bate, M. 1996, in preparation
- Benz, W. 1990, in *The Numerical Modeling of Nonlinear Stellar Pulsations*, ed. J.R. Buchler, Kluwer Academic Publishers, Dordrecht, p. 269
- Cannizzo, J. K. 1993, ApJ, 419, 318
- Davies, M.B., Ruffert, M., Benz W., & Müller, E. A&A, 272, 430
- Dgani, R., Livio, M., & Soker, N. 1989, ApJ, 336, 350
- Frank, J., King, A. R., & Lasota, J. P. 1987, A&A, 178, 137
- Hellier, C., & Livio, M. 1994, ApJ, 424, L57
- Hirose, M., Osaki, Y., & Minishige, S. 1991, PASJ, 43, 809
- Kaitchuck, R. H., Schlegel, E. M., Honeycutt, R. K., Horne, K., Marsh, T. M., White, J. C., II, & Mansperger, C. S. 1994, ApJS, 93, 519
- Krolik, J. H., McKee, C. F., & Tarter, C. B. 1981, ApJ, 249, 422
- Lanzafame, G., Belvedere, G., & Molteni, D. 1994a, MNRAS, 258, 152
- Lanzafame, G., Belvedere, G., & Molteni, D. 1994b, MNRAS, 267, 312
- Lin, D. N. C., & Papaloizou, J. 1979, MNRAS, 186, 799
- Lin, D. N. C., & Pringle, J. E. 1976, in *Structure and Evolution of Close Binary Systems*, ed. P. Eggleton, D Reidel, Dordrecht, p. 237
- Livio, M. 1993, in *Accretion Disks in Compact Stellar Systems*, ed. J. C. Wheeler (Singapore: World Scientific), p. 243
- Livio, M. 1994, in *Interacting Binaries*, Saas-Fee Advanced Course 22, eds. H. Nussbaumer & A. Orr, Springer-Verlag, Berlin Heidelberg, p. 142
- Livio, M., Soker, N., & Dgani, R. 1986, ApJ, 305, 267
- Long, K. S., Mauche, C. W., Raymond, J. C., Szkody, P., & Mattei, J. A. 1996, ApJ, in press
- Lubow, S. H. 1989, ApJ, 340, 1064
- Lubow, S. H. 1991, ApJ, 381, 268
- Lubow, S. H., & Shu, F. H. 1975, ApJ, 198, 383
- Lubow, S. H., & Shu, F. H. 1976, ApJ, 207, L53
- Marsh, T. R., Horne, K. 1988, MNRAS, 235, 269
- Mason, K. O. 1989, in *Proc. 23rd ESLAB Symp. on Two-Topics in X-Ray Astronomy*, ESA SP-296, p. 113

- Monaghan, J. J. 1992, *ARA&A*, 30, 543
- Murray, J. R. 1996, *MNRAS* in press
- Paczyński, B. 1977, *ApJ*, 216, 822
- Papaloizou, J., & Pringle, J. E., 1977, *MNRAS*, 181, 441
- Pringle, J. E. 1981, *ARA&A*, 19, 137
- Pringle, J. E., Verbunt, F., & Wade, R. A. 1986, *MNRAS*, 221, 169
- Rozyczka, M. & Schwarzenberg-Czerny, A. 1987, *Acta Astron.*, 37, 141
- Schandl, S., Meyer-Hofmeister, E., & Meyer, F. 1996, *A&A*, submitted
- Shakura, N.I., & Sunyaev, R.A. 1973, *A&A*, 24, 337
- Szkody, P., Long, K. S., Sion, E. M., & Raymond, J. C. 1996, *ApJ*, in press
- Warren, J. K., Sirk, M. M., & Vallergera, J. V. 1995, *ApJ*, 445, 909
- White, N. E. & Holt, S. S. 1982, *ApJ*, 257, 318
- White, N. E., Arnaud, K., Day, C. S. R., Ebisawa, K., Gotthelf, E. V., Mukai, K., Soong, Y., Yaqoob, T., & Antunes, A. 1994, *PASJ*, 46, L97
- White, N. E., Nagase, F., & Parmar, A. N. 1995, in *X-Ray Binaries*, eds. W. H. G. Lewin, J. van Paralijs, & E. P. J. vanden Heuvel (Cambridge: Cambridge University Press), p. 1
- Whitehurst, R. 1988a, *MNRAS*, 232, 35
- Whitehurst, R. 1988b, *MNRAS*, 233, 529